Size Dependence of Conjugation of Amyloid Beta Protein on Gold Colloidal Nanoparticles' Surfaces

K. Yokoyama, D. Sri Hartati, W. Tsang, N. M. Briglio and J. E. MacCormac

The State University of New York Geneseo College, Geneseo, NY, USA, yokoyama@geneseo.edu

ABSTRACT

Fibrillogenesis of amyloid beta (Aβ) monomers is a hallmark of Alzheimer's disease. The initial stage of this process involves intermediates of Aβ aggregates; which have been the focus of many previous fibrillogenesis studies. We discovered that gold colloidal nanoparticles with an average diameter of 20 nm, coated with $A\beta_{1\text{-}40}$, exhibited a reversible aggregation process between pH 4 and pH 10, while the rest of the tested gold colloidal particles did not. This discovery contains a significant implication for the initial step of fibrillogenesis where intermediates of fibrillogenesis exist, while the form of the intermediate is still controversial. Our information on a possible intermediate involves a metal surface which is intended to utilize the nano-scale interfacial environment geometrically mimicking a human membrane or brain cells.

Keywords: gold colloids, amyloid beta, Alzheimer's disease, pH dependence, surface adsorption

1 BACKGROUND

Pathologically, a key hallmark of the neuritic and cerebrovascular amyloid in Alzheimer's disease is the formation of insoluble fibrillar deposits of amyloid β-peptides (Aβ) as both diffuse and senile amyloid plaque that invades the brain's seat of memory and cognition before spreading to other areas. The 42- and 40-residue, $A\beta_{1\text{-}42}$ and $A\beta_{1\text{-}40}$ are capable of assembling into 60–100Å diameter β-sheet fibrils. Highly hydrophobic $A\beta_{1\text{-}42}$ is implicated in amyloid fibril nucleation, while the more soluble $A\beta_{1\text{-}40}$ is the main form circulating in normal plasma and cerebrospinal fluid. The fibrillogenesis is considered to be a nucleation-dependent polymerization process and progresses as a polymerization process originating from a unit nucleus formed by certain numbers of monomeric Aβ, involving the initial formation of a seeding aggregate that establishes the amyloid fibril lattice, followed by the elongation of the fibril by the sequential addition of subunits. An initial stage involving a soluble Aβ complex has been regarded as a pathologically important step and a key to onset of the following aggregation, and the existence of metastable folding intermediates, *i.e.*, oligomer form, for a folding pathway has been suggested and detected. Such folding intermediates are expected to be readily reversible, yet may serve as precursors for fibril nucleation and/or mediate fibril growth. (See Figure 1)

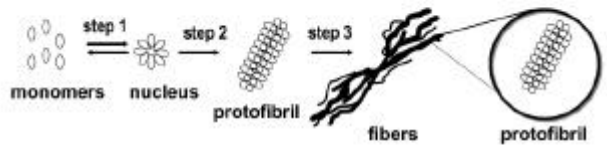

Figure 1. A model of fibrillogenesis. Fibrillogenesis is considered to be a nucleation-dependent polymerization process. In step1, monomeric Aβ forms nuclei from which protofibrils emanate (step 2). These protofibrils give rise to fill-length fibers (step 3).

The Aβ placed at the human membrane or brain cells must induce the fibrillogenesis differently from the one which possesses maximum degrees of freedom in the solution. A lack of information on the behavior of Aβ at the interface prevents us from obtaining a clear picture of the structural confirmation of the intermediate appearing at step 1 in Figure 1. In order to systematically investigate Aβ situated at an interface, we utilized an externally size-controllable interfacial surface of gold colloidal nanoparticles to manipulate the structure of the adsorbed protein on that surface. Zare's group utilized Cytochrome-c (Cyt-*c*) as a representative case to demonstrate that the conformational change on the gold colloidal nanoparticle can be fully specified through spectroscopic information.[1] Following their work, we recently discovered self-assembled Aβ on spherical gold nanoparticles, and confirmed the pH-induced conformational change using absorption spectroscopy.

2 EXPERIMENTAL

The gold and silver colloidal nanoparticles with various diameters ranging from 5 nm to 100 nm were purchased from Ted Pella Inc. (Redding, CA), and various amyloid beta (Aβ) proteins were obtained from American Peptide Corp. (Sunnyvale, CA). The Aβ proteins were dissolved in deionized distilled water in order to prevent the destabilization of colloidal particles by ionic species of the buffer solutions. The ratio of 1000 : 1 between Aβ and gold colloid was selected as the optimum ratio in this study, where the concentration of gold colloid particles in this

experiment was 0.19 nM and the concentration of the Aβ solution was 0.19 μM.

The pH change from 7 to 2 was by drop-wise addition of hydrochloric acid (HCl) and that of between 7 and 10 was by addition of sodium hydroxide (NaOH) with step of roughly pH 0.3. The reversibility of the color change of the solution was investigated for all Aβ solutions between pH 4 and pH 10 by adding an adequate amount of base or acid solution as its absorption spectrum was monitored.

The image of this film surface was examined by Atomic Force Microscopy (AFM) with tapping mode in a laboratory at SUNY-Albany. The mixture of $A\beta_{1-40}$ and gold colloidal particles of 20 nm of size (pH of 4, 7, and 10) was disposed onto the graphite and dried to compose a film.

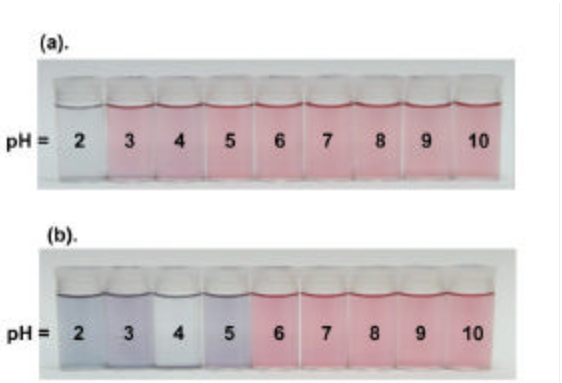

Figure 2. (a) The color of the solution of gold colloidal nanoparticle with size 20 nm at various pHs. (b)The color of $A\beta_{1-40}$-coated nanoparticle solutions at different pHs.

3 RESULTS

3.1 pH dependence

The bare gold nanoparticle solutions show almost no change from the original color except for pH 2, whereas the $A\beta_{1-40}$-coated particles displayed obvious color variation around pH 5 or smaller pHs. (See Figure 2)

All the absorption bands in the range of 400 to 800 nm were fit to a Gaussian profile using the peak-fit-module of ORIGIN (Version 7.0). When the band component consisted of two parts, the peak position, λ_{peak}, was determined by the following method.

$$l_{peak} = \sum_{i=1}^{n} a_i l_i = a_1 l_1 + a_2 l_2 \qquad (1)$$

where λ_i and a_i represent the peak position and a fraction of the i^{th} component band, and most of the bands observed in our study were fully analyzed with two components or one component with a large background band with a maximum at 350±50 nm. The position of the peaks between 400 and 800 nm as a function of the pH values are plotted in Figure 3 (b). In our analysis, an index showing color change as a function of pH was defined as (pH_o), which was extracted by an analytical formula characterized by a growth/sigmoidal function, a Boltzmann -like formula:

$$l_{peak}(pH) = [l_{\min} - l_{\max}]/[1+\exp(pH - pH_o)dpH] + l_{\max} \qquad (2)$$

The $\lambda_{\min}$ and $\lambda_{\max}$ are the minimum and maximum of the band peak positions between 400 nm and 800 nm. The pH_o is the pH value when $\lambda_{peak} = (\lambda_{\min} + \lambda_{\max})/2$. The *d*pH is defined as: $d\text{pH} = (\lambda_{\max} - \lambda_{\min})/4\,\lambda_{peak}^{(1)}$, where $\lambda_{peak}^{(1)}$ is the first derivative of the $\lambda_{peak}(\text{pH})$.

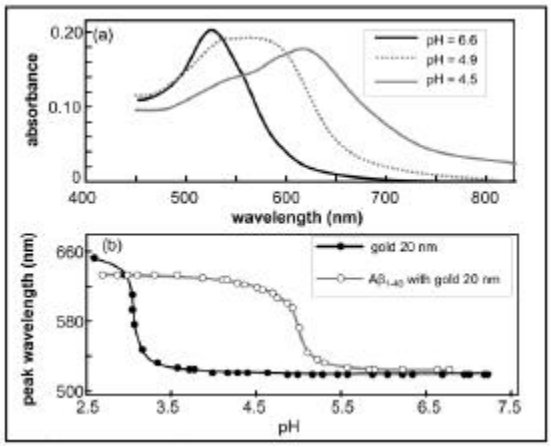

Figure 3. (a) The three representative absorption spectra of gold 20 nm nanoparticles and $A\beta_{1-40}$ solutions between pH 4.5 and pH 6.6. (b) The peak position of the absorption spectrum in the region between 400 nm and 800 nm.

3.2 Sequence dependence

We have chosen sequences to test the role of different functional portions of the Aβ. The $A\beta_{1-11}$, $A\beta_{12-28}$ or $A\beta_{31-35}$ segments exhibit a hydrophilic tail, both hydrophilic/hydrophobic tail, and hydrophobic tail of $A\beta_{1-40}$ sequences, respectively. At the particular sequence Lys-Leu-Val-Phe-Phe, $A\beta_{16-20}$ is known to be critical for Aβ-Aβ binding and fibril formation,[2] thus, the importance of the above sequence $A\beta_{16-20}$ to a fibrillogenesis will be investigated from $A\beta_{12-28}$ and $A\beta_{1-40}$.

The obtained λ_{max} and pH_o values for various Aβ sequences are listed in Table 1. (The pH_o for bare gold nanoparticles was determined to be 3.09±0.02.) The pH_o value showed a slight dependence on the sequence of Aβ as most of the Aβ protein mixture showed the transitions around pH 5. However, only $A\beta_{1-42}$ has a relatively low pH value for its color change. A close match between the values of $A\beta_{1-11}$ (pH_o= 4.56±0.03) and $A\beta_{31-35}$ (pH_o= 4.68±0.05) was observed. While the peak position at the higher pHs, λ_{min}, were the same for all sequences (528±3

nm), the peak position at the lower pH, λ_{max}, showed a dependence on the sequences. The aggregation process is estimated to be enhanced when pH is close to its isoelectric point (pI). The pI of $A\beta_{1-40}$ is reported to be about 5.5.[3]

Sequence	$A\beta_{1-40}$	$A\beta_{1-11}$	$A\beta_{12-28}$	$A\beta_{31-35}$
pI	5.2	4.1	7.9	6
pH_o	4.96(2)	4.56(3)	5.27(2)	4.68(5)
λ_{max} (nm)	611(2)	628(3)	599(4)	628(6)

Table 1. The summary of parameters for various Aβ adsorbed on the surface of gold nanoparticle.

3.3 Size dependence

The pH dependence of the peak shift as well as the reversibility of the color change was investigated for the various gold colloidal sizes from 5 to 100 nm with $A\beta_{1-40}$. The concentration ratio between Aβ and gold colloid was maintained as 1000 : 1. While the value of pH_o slightly increased as a function of gold colloidal size, the Aβ adsorbed on the gold colloid surface exhibited a peculiar size dependence in pH as shown in Figure 4 where the pH_o peaked at the gold colloid of 40 nm and 80 nm.

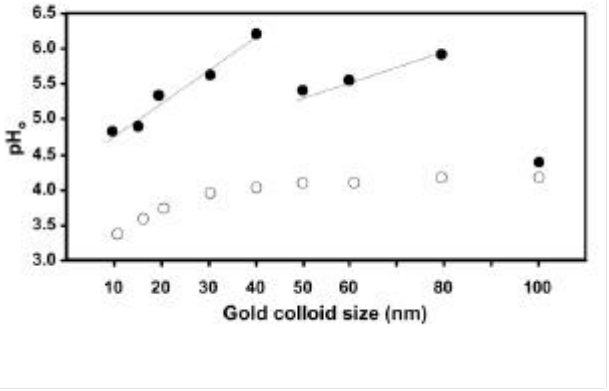

Figure 4. The size dependence of the pH_o. The open circles indicate the values for gold colloids only, and the black circles are for $A\beta_{1-40}$ coated gold colloids. The line was given to clarify the observed trend.

3.4 AFM study

AFM images were collected for those originating from the $A\beta_{1-40}$ conjugated gold colloidal nanoparticles of 20 nm prepared at pH 4, pH 7 and pH 10, respectively. (See Figure 5) These solutions correspond to the sample shown in the Figure 2, where a pink color was observed for pH 7 and 10, while a blue color was observed for pH 4. The graphite surface showed a sign of low sticking coefficient for gold colloid so that gold particles tended to segregate above the film. In pH 4, the gold particles laid above the non continuous layer, which can be a β-pleated sheet. The gold nanoparticles agglomated into a size of 39 nm. A similar situation was seen at pH 7, where a layer of the proteins are seen with gold nanoparticles above the layer with agglomates of 23 nm. However, the morphology of the proteins changed into a more fiber like formation which bridged the largely agglomated gold colloid particles (55 nm) at pH 10.

Overall, the images given for these solutions were drastically different from those taken for bare gold colloid and $A\beta_{1-40}$ only. However, there were no significant differences found among those images. The homogeneous sheet was formed beneath the gold colloid particles, and the gold colloid particles were placed over the top of this sheet layer indicating that the gold colloid did not stick well with the graphite surface. The morphology of $A\beta_{1-40}$ was rather string like conformation for pH 10 suggesting that the conformation of the protein is different in these two pH values. The homogeneous sheet observed in pH 7 and 4 can be assigned as β-sheet. The string like form observed in pH 10 can still be a β-sheet which is discontinuous. However, the morphology due to the gold colloid can not be fully concluded due to low sticking coefficient between gold colloid and graphite surface.

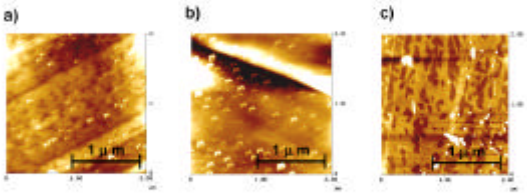

Figure 5. The AFM image of $A\beta_{1-40}$ conjugated on the surface of gold colloid 20 nm on the surface of graphite. The condition of deposited solution was a)pH 4, b) pH 7, and c) pH 10.

3.5 Adsorption on the silver colloid

The conjugation of $A\beta_{1-40}$ with silver gold colloid with the size of 20 nm, 40 nm and 60 nm was conducted in order to investigate the effect of the change in the metal surface potential.(Figure 6) The peak of the surface plasmon resonance is around 400 nm at the higher pHs (>pH7), and the peak position shifted to ~550 nm as the pH was lowered (<pH 4). The peak wavelength at the lower pH side increased as a function of size of the colloid for both bare silver colloids and $A\beta_{1-40}$ coated silver colloids. However, the pH_o values for bare silver colloid reside around pH_o= 4.5, while the pH_o values for the $A\beta_{1-40}$ adsorbed silver colloids showed a significant shift to around pH_o =5.0. The change in pH_o observed in $A\beta_{1-40}$ coated gold colloid was onto the higher pH as the $A\beta_{1-40}$ was adsorbed on the gold colloid surface. In the same way, the change of pH_o observed on $A\beta_{1-40}$ coated silver colloids was also onto the higher pH. However the degree of change in pH_o was

larger in the case of gold colloid. This result is consistent with the fact that gold metal is *softer* according hard-soft acid base theory.

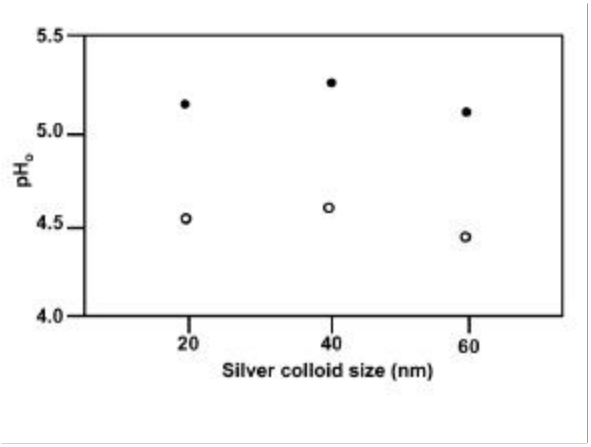

Figure 6. The size dependence of the pH_o. The open circles indicate the values for silver colloids only, and the black circles are for $A\beta_{1-40}$ coated silver colloids.

3.6 Reversibility

The reversibility of the color transition was examined by repeatedly varying pH values of the solution between pH 4 and 10 by addition of acid or base solutions to a sample mixture. A corresponding color change was clearly observed in only $A\beta_{1-40}$ coated gold colloidal particles with 20 nm size. (Figure 7-b) This color change could be repeated at least 10 times, though no sign of termination of the reversible process was detected. The color change in the reversible process was not between pure blue and red, rather it was between purple and red. The peak at pH 10 shifts gradually to 560$\pm$1 nm from 528 nm as the repetition number of the pH change increased, while the absorption band at pH 4 appears around 580 nm, where it consists of two peaks where one centers around 528$\pm$1 nm and the other centers at 600 nm. The reversible change was not observed in the rest of the gold colloid sizes. (Figure 7-a)

4 CONCLUSIONS

A reversible process took place only in $A\beta_{1-40}$ associated with the aggregation of gold colloidal nanoparticles of 20 nm size between pH 4 and 10, which strongly suggests the structural change under different pH can be reversibly conformed. Quite significantly, this reversible process implies a correspondence to a reversible stage of initial fibrillogenesis and may involve a structural conformation of the intermediate of the fibrillogenesis.

While the AFM image exhibited the sheet-like formation of the Aβ aggregate indicating the formation of a β sheet in our experimental condition, it did not exhibited a convincing evidence for the cause of color change at different pHs. Therefore, the presence of the water or solvent is considered to play a key role in conforming the aggregation of the Aβ-gold colloid.

The pH_o value showed a trend maximizing at 40 nm (or 80 nm) for the $A\beta_{1-40}$ coated gold and silver colloids. This suggests that surface area provided by the 40 nm or multiples of 40 nm size can be associated with a specific geometrical restriction for the aggregates of $A\beta_{1-40}$ monomers.

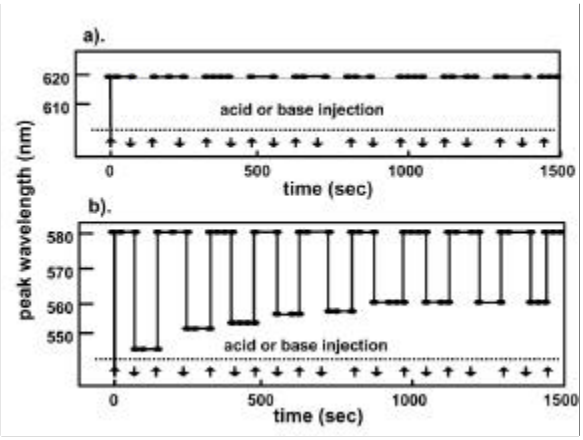

Figure 7. A demonstration of the color change reversibility seen in (a) gold colloidal particles 50 nm and $A\beta_{1-40}$ and (b) gold colloidal particles 20 nm and $A\beta_{1-40}$ solutions. The peak position of the absorption band was plotted as a function of time. The upward and downward arrows indicate the time adjusting the pH of the solution at pH 4 and pH 10, respectively.

REFERENCES

[1] S. Chah, C. V. Kumar, M. R. Hammond, and R. N. Zare, "Denaturation and renaturation of self-assembled yeast iso-1-cytochrome c on Au,," Anal. Chem. 76, 2112-2117 (2004).

[2] L. O. Tjernberg and C. Nordstedt, "Arrest of beta-amyloid fibril formation by a pentapeptide ligand," J. Biol. Chem. 271, 8545-8548 (1996).

[3] Y. Fezoui, D. M. Hartley, J. D. Harper, R. Khurana, D. M. Walsh, M. M. Condron, D. J. Selkoe, J. Lansbury, P. T., A. L. Fink, and D. B. Teplow, "An improved method of preparing the amyloid beta-protein for fibrillogenesis and neurotoxicity experiments," Amyloid: Int. J. Exp. Clin. Invest. 7, 166-178 (2000).